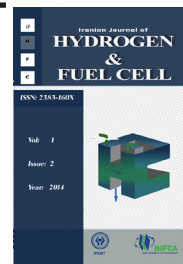


Iranian Journal of Hydrogen & Fuel Cell

IJHFC

Journal homepage://ijhfc.irost.ir



Modeling of measurement error in refractive index determination of fuel cell using neural network and genetic algorithm

Saeed Olyae^{1,*}, Reza Ebrahimpour², Somayeh Esfandeh¹

¹ Nano-photonics and Optoelectronics Research Laboratory (NORLab), Faculty of Electrical and Computer Engineering, Shahid Rajaei Teacher Training University, Lavizan, 16788-15811, Tehran, Iran

² Brain & Intelligent Systems Research Lab (BISLab), Faculty of Electrical and Computer Engineering, Shahid Rajaei Teacher Training University, Tehran, Iran

Article Information

Article History:

Received:

28 February 2014

Received in revised form:

31 August 2014

Accepted:

1 September 2014

Keywords

Fuel cell

Genetic algorithm

Heterodyne interferometer

Multi-layer perceptrons

Nonlinearity error

Refractive index

Stacked generalization

Abstract

In this paper, a method for determination of refractive index in membrane of fuel cell on the basis of three-longitudinal-mode laser heterodyne interferometer is presented. The optical path difference between the target and reference paths is fixed and phase shift is then calculated in terms of refractive index shift. The measurement accuracy of this system is limited by nonlinearity error. In this study, nonlinearity error is modeled by multi-layer perceptrons (MLPs) and stacked generalization method (Stacking), using two learning methods; back propagation (BP) and genetic algorithm. Training neural networks with genetic algorithm improves modeling of nonlinearity error in this system. In the proposed technique, a real code version of genetic algorithm is used. Parameters and genetic operators are set and designed accurately. The results indicate that the nonlinearity error can be effectively modeled by training the stacking with the genetic algorithm which has minimum mean square error (MSE).

1. Introduction

The use of fuel cell is a means of producing energy, such as electricity and heat. Fuel cell is an electrochemical device for transmitting electrochemical energy to useful electrical energy [1]. We use fuel cell in order to produce electrical energy in power plants, portable

devices, automobiles, etc. Fuel cell is an important technology for producing clean energy with high efficiency. It consists of an anode, a cathode, and two current collectors separated by a thin membrane [2]. Operation of fuel cell systems directly depends on the water content in the membrane. High water content increases the efficiency of fuel cell; however, if it is

*Corresponding author Email: s_olyae@srttu.edu

too high, then some problems occur, including: swell, mechanical pressure, and destruction of fuel cell membrane [3]. Density and refractive index in membrane are commensurate together, thus estimating the refractive index helps measuring the water content in fuel cell membrane.

There are many developed methods for imaging water content with magnetic resonance imaging, neutron imaging, and optical fluorescence spectroscopy [4, 5]. All of these methods are expensive to run, or have weak resolution and are very complicated and time-consuming. Therefore, interferometry methods are attractive and favored by researchers to measure refractive index in recent years. Mach-Zehnder and two-longitudinal-mode laser heterodyne interferometers are used for recognizing variation of water content percentage and duration of penetrating process in fuel cell [6, 7].

We use three-longitudinal-mode laser heterodyne interferometer rather than two-mode to obtain higher resolution capabilities. Three-longitudinal-mode laser heterodyne interferometer has improved with high sensitivity, which measures refractive index shift versus variation of water content in fuel cell membrane. Nonlinearity error in heterodyne interferometer limits accuracy of measurement of refractive index. This error is due to non-ideal laser polarization, optical devices, and electronic measurement system. Thus, modeling and analyzing of measurement errors are very important. Researchers have worked for modeling, calculating, and finally compensation of nonlinearity by using complicated calculation analysis [8-10]. Nowadays, the neural networks play an important role in modeling of nonlinearity error in laser interferometer [11, 12]. Olyae et al. have modeled the nonlinearity of two-mode heterodyne interferometer by using MLPs and radial basis function, and Stacking method [13].

When nonlinearity error is modeled by MLPs and Stacking using back propagation (BP) as their learning algorithm, it cannot offer a good model. Gradient descent based techniques usually tend to stick in local minima and it depends on the shape of the error surface exactly. Therefore, replacing it with genetic algorithm

can be very useful.

In this paper, nonlinearity error due to ellipticity and non-orthogonality of input polarized light of three-mode heterodyne is modeled. This modeling has been done in order to have more accurate system for measuring refractive index shift due to variation of water content in fuel cell. The nonlinearity error is modeled by MLPs, Stacking method, trained MLPs with genetic algorithm (we call it MLPs-GA) and trained Stacking with genetic algorithm (we call it Stacking-GA). Their performances are also compared. MLPs-GA and Stacking-GA methods avoid sticking in local minima and they search the whole space of the problem. Thus, these two methods are expected to have better results for measuring refractive index shift in fuel cell.

Outline of this article is as follows: In the next part, the refractive index shift due to the variation of water content in the fuel cell membrane is discussed based on three-longitudinal-mode laser heterodyne interferometer. In the third part, the modeling of nonlinearity error for measurement of the refractive index shift is described by using MLPs and Stacking. The basis of genetic algorithm is presented in the fourth part. In the fifth part, MLPs-GA and Stacking-GA methods for modeling of nonlinearity error are introduced. Finally, in the last part simulation results are drawn.

2. Measurement of the refractive index

Three-longitudinal-mode heterodyne interferometer has higher accuracy compared to two-mode interferometer. The structure of three-longitudinal-mode laser heterodyne interferometer for high accuracy measuring of refractive index shift in fuel cell is shown in Fig. 1.

The laser beam is emerged by the stabilized He-Ne laser with 632.8 nm wavelength. The beam is divided into two paths by beam splitter, reference and target paths. Then, according to polarizations, the light is divided into two paths in x- and y-directions by using polarizing beam splitter (PBS). The reflected beams

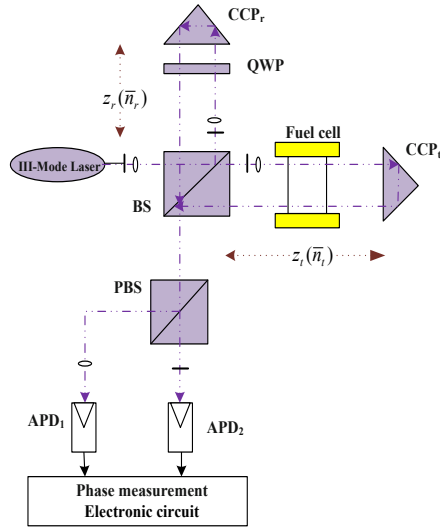


Fig. 1. The schematic representation of a three-mode laser heterodyne interferometer. QWP: quarter-wave plate, CCP: corner cube prism, PBS: polarizing beam splitter, APD: avalanche photodiode, BS: beam splitter.

are interfered and detected by two avalanche photodiodes. The outputs of the two avalanche photodiodes are sent to signal conditioner and digital signal processing circuit to detect phase shift resulting from the changes in refractive index of the fuel cell [13]. The electrical fields of three-longitudinal-mode laser output are written as:

$$E_{v_1} = \begin{bmatrix} 1 \\ |\alpha| \exp(i\varphi_\alpha) \end{bmatrix} \exp i(2\pi\nu_1 t) \quad (1)$$

$$E_{v_2} = \begin{bmatrix} |\beta| \exp(i\varphi_\beta) \\ 1 \end{bmatrix} \exp i(2\pi\nu_2 t) \quad (2)$$

$$E_{v_3} = \begin{bmatrix} 1 \\ |\alpha| \exp(i\varphi_\alpha) \end{bmatrix} \exp i(2\pi\nu_3) \quad (3)$$

In this equation ν_1 , ν_2 and ν_3 are the optical frequencies of three modes and $|\alpha| \exp(i\varphi_\alpha)$ and $|\beta| \exp(i\varphi_\beta)$ are made by ellipticity polarization and non-orthogonality of input polarized light. It can be easily proved that the two photocurrents of avalanche photodiodes are gained by calculating electric fields square from the following equations:

$$I_{APD_1} = k \cos(2\pi\nu_b t - 2\Delta\psi + \Psi_1) \quad (4)$$

$$I_{APD_2} = k \cos(2\pi\nu_b t + 2\Delta\psi + \Psi_2) \quad (5)$$

where, k is a constant value and $\nu_{bL} = \nu_2 - \nu_1$, $\nu_{bH} = \nu_3 - \nu_2$ and $\nu_b = \nu_{bH} - \nu_{bL}$ are the intermode beat frequencies. Also, Ψ_1 and Ψ_2 are the phase shift nonlinearities and ψ_r and ψ_t are phase shifts in the reference and target paths, respectively [7]. The free-error phase between the target and reference paths resulting from the refractive index shift of fuel cell is denoted by $\Delta\psi$ which can be given as:

$$\Delta\psi = \psi_t - \psi_r = (4\pi z / \lambda) \Delta n \quad (6)$$

where, $|\bar{n}_t - \bar{n}_r| = \Delta n$ is the difference in refractive index due to the change of water content of the fuel cell membrane, λ the wavelength, and z the optical path difference (OPD). The phase difference between the two measured output signals is derived as follows:

$$\Delta\Phi = 4\Delta\psi (\Psi_1 - \Psi_2) \quad (7)$$

The first part determines twice-increased resolution compared with two-longitudinal-mode heterodyne interferometer and the second part ($\Psi_{nl} = \Psi_1 - \Psi_2$), is the nonlinearity error. While there is a linear relation between the measured phase difference and refractive index, the refractive index shift is obtained by measuring the phase shift as:

$$\Delta n = \frac{\lambda}{16\pi z} (\Delta\Phi + \Psi_{nl}) \quad (8)$$

For accurate measurement of refractive index, nonlinearity phase should be eliminated. In the next part, the nonlinearity errors are modeled with MLPs and Stacking neural networks using two different learning methods: back propagation and genetic algorithm.

3. Neural networks

3.1. Multi-layer perceptrons (MLPs)

Modeling of the nonlinearity error in three-longitudinal-mode laser heterodyne interferometer using neural network is shown in Fig. 2. We use back propagation algorithm for training the MLPs. The MLPs include an input layer, a hidden layer, and an output layer, as shown in Fig. 3. The MLPs can have more than one hidden layer, but it has been theoretically proved that only one hidden layer is sufficient for neural networks to estimate any complex nonlinear function [14]. The

includes two neurons in input layer, 12 neurons in the hidden layer and one neuron in the output layer. The learning process finds the optimum value of connection weights and biases of the input-hidden layer and hidden-output layer. Output of each neuron which belongs to hidden layer is shown in Fig. 4. The output of each neuron is gained with summation over the multiplication of each input and its corresponding weight, and finally, the result is passed through a nonlinear activation function (transfer function). The sigmoid tangent activation function $f(x)$ is used to transfer the values of input layer neurons to

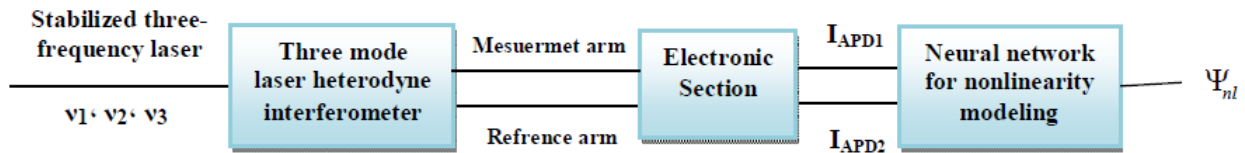


Fig. 2. Modeling of the nonlinearity error in the three-longitudinal-mode laser heterodyne interferometer by using neural network.

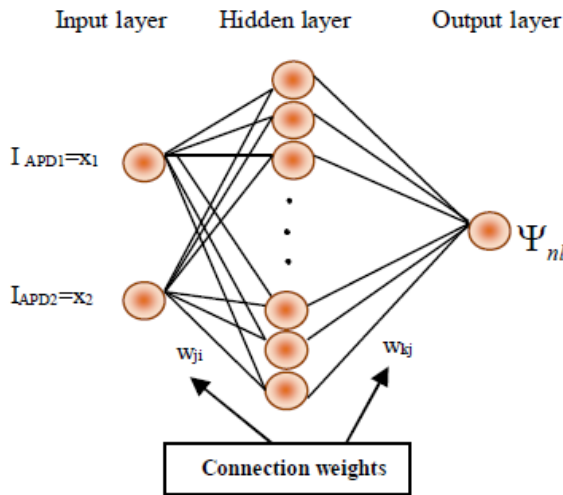


Fig. 3. The structure of MLPS network for modeling of nonlinearity error.

output currents of two avalanche photodiodes (APD1, APD2) as input and nonlinearity error heterodyne interferometer (Ψ_{nl}) as desired output are considered for MLPs neural network.

Number of neurons in the hidden layer is obtained by trial and error. The structure of the neural network

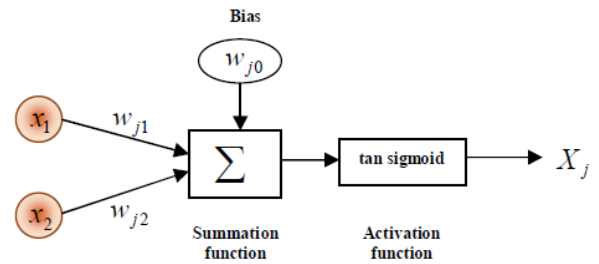


Fig. 4. The relation between input and output of hidden layer neuron.

output of hidden layer neurons to the output layer. The output neurons of the hidden and last layers are calculated by Eqs. (9) and (10) [15]:

$$X_j = f\left(\sum_{i=1}^2 x_i w_{ji} + w_{j0}\right) \tag{9}$$

$$\hat{\Psi}_{nl} = p\left(\sum_{j=1}^{12} X_j w_{kj} + w_{k0}\right) \tag{10}$$

where x_i is a variable input, w_{ji} connection weight between hidden and input neurons, w_{kj} connection weight between output and hidden neurons, w_{j0} and w_{k0} are biases for the j^{th} and k^{th} neuron respectively, i a number of neurons for input, j a number of neurons for the hidden layer, and k the number of output neurons. Output of neural network, $\hat{\Psi}_{nl}$, is compared with the desired output, Ψ_{nl} , in the training phase, and the error in the form of mean square error (MSE) is calculated for all data. The MSE function is derived from the following equation:

$$MSE = \frac{1}{n} \sum_{p=1}^n [(\Psi_{nl})_p - (\hat{\Psi}_{nl})_p]^2 \quad (11)$$

where n is the number of data in the training phase. The purpose is to reduce the amount of errors. The adjustment applied to the synaptic weight is calculated as follows:

$$\Delta w_{ji} = -\eta \frac{\partial MSE}{\partial w_{ji}} \quad (12)$$

where, η is the learning rate, and is selected carefully. Through the training phase, the neural network learns and generalizes nonlinear relationship and maps the input to the output.

3.2. Stacked Generalization method

Stacked Generalization method or Stacking has been proposed by Wolpert in 1992 [16]. It is a combined method for training input data, such that the system gets more generalizability. General framework of this method includes two levels as shown in Fig. 5.

The first level (called level-0) is a set of k divers' neural network and each of them are called a base classifier. Each classifier is trained with original data. Then, the output of the zero level is used as the input of the next level (called level-1). As shown in Fig. 5, N_1^0 to N_k^0 stand for k networks sorted as first layer and their output is combined by the N_1^1 network at level-1. During the training process, the combiner learns optimum weights for the combination of base classifiers outputs. Using such a combination method,

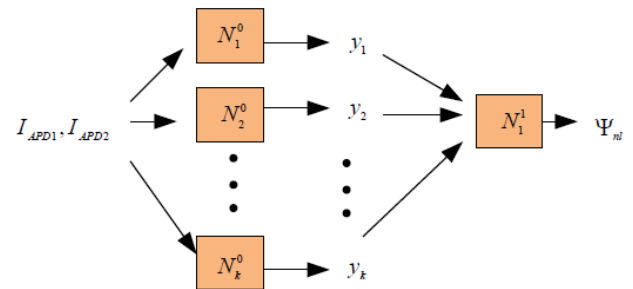


Fig. 5. Stacking method for modeling of nonlinearity error in the refractive index determination system of fuel cell.

we will reach the results much better than when using each single classifiers. Four MLPs networks with a hidden layer are used at level-0 and one MLP is used at level-1 for nonlinearity modeling of three-mode heterodyne interferometer in measurement of refractive index shift in fuel cell.

4. Genetic algorithms

Genetic algorithm (GA) is a member of large family of evolutionary algorithms that has grown rapidly in the field of artificial intelligence. For the first time, GA was introduced by John Holland in early 1970 [17]. This algorithm is a powerful optimization tool, inspired of natural genetic and Darwin's evolutionary theory. This algorithm operates under the genetic laws and natural selection. It is an effective search method for problems with complex space [18]. In order to use the genetic algorithms following steps should be considered:

- 1- Chromosome representation and initialization,
 - 2- Calculate fitness function (evaluating chromosome),
 - 3- Using evolutionary operators such as selection, crossover, and mutation,
 - 4- Replacement (select next generation) and termination criteria.
- GA is improving the fitness of population using aforementioned operators. The GA Learning process is shown in Fig. 6.

5. Training of MLPs and Stacking with genetic algorithms

When the nonlinearity error is modeled with MLPs and Stacking, in order to measure the refractive index shift in fuel cell with three mode heterodyne interferometer, weights of the network usually is learnt by the back propagation algorithm (BP) based on the gradient descent algorithm. Despite the popularity of these techniques for training neural network, it has

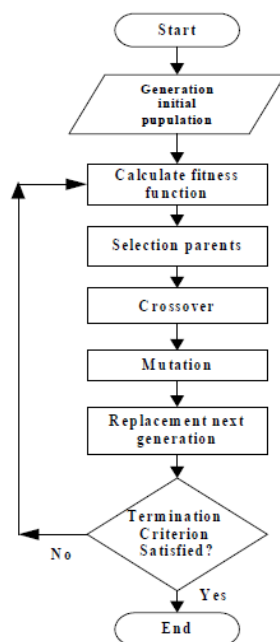


Fig. 6: The learning process flowchart using the GA.

some drawbacks. It depends on the shape of the error surface exactly. Gradient descent based techniques, usually tends to stick in local minima [19]. Thus, the nonlinearity error cannot be modeled well. In this paper, we use genetic algorithm instead of gradient descent algorithm in MLPs and Stacking. Our results depict that the refractive index of the fuel cell will be determined more accurately.

Genetic algorithm can be used in two different ways for training neural networks: 1- Weights optimization and 2- Structure and topology optimization [20]. We use the first approach in our neural network learning process. The proposed methods are explained in the following parts.

5.1. Chromosome representation and initialization

In problems with large number of variables, we can avoid the complexity by using the real number for chromosomes presentation instead of the binary form. In addition, in such problems, convergence of genetic algorithm by using the binary structure is very controversial. In this paper, we use the real number form for chromosome representation and its genetic operators to train the MLPs and Stacking. The initial population is selected randomly.

5.1.1. Chromosome representation in the MLPs training phase

In this part, we consider the MLPs that have been described in section 3.1. Connection weights and biases are trained by using genetic algorithms. Our MLPs network has two neurons in the input layer, 12 neurons in the hidden layer and one neuron in output layer. Thus, the total number of weights and biases are 49. All these connection weights and biases between layers of network are represented as genes of each chromosome. Thus, each chromosome with 49 genes is represented as one set of weight.

5.1.2. Chromosome representation in the Stacking training phase

The Stacking method is presented in 3.2. It contains of one MLPs network at level-1 and all its weights are trained with the BP algorithm. In the proposed method this algorithm is replaced by GA to overcome problems of gradient descent algorithm in MLPs network. The outputs of 4 networks in level-0 are used as inputs of the second level MLPs (level-1), and then the final output is the nonlinearity of interferometer in measurement of refractive index shift in fuel cell. The MLPs of level-1 has four neurons in the input layer, 12 neurons in the hidden layer and one neuron in the output layer. This structure includes 73 weights and biases, which present 73 genes in each chromosome. It should be noted that each chromosome just includes connection weights and biases and it does not include

any topology and other structural information.

5.2. Calculation of fitness function

Evaluation of each set of connection weights (each chromosome) is carried out by making corresponding neural network structure. Mean square error between the actual output and target is chosen as fitness function that is given as:

$$MSE = 10 * \log\left(\frac{1}{n} \sum_{p=1}^n [(\Psi_{nl})_p - (\hat{\Psi}_{nl})_p]^2\right) \quad (13)$$

5.3. Evolutionary operators

5.3.1. Selection

In GA, selection of individuals for produce successive generations has a vital role. In this paper, we use stochastic universal sampling (SUS) method. SUS is a sampling method which implements selection proportional to the fitness. It is proposed to overcome some of the problems of roulette wheel sampling method. In roulette wheel selection method, the wheel turns N times; N is population size. In each time, each chromosome that its sector was faced against marker is selected for generation. In SUS method, the wheel runs only once and hence it is used to choose N parent from N marker placed in the same distance from each other. After the wheel stops, each chromosome is selected on the basis of the number of the marker placed against it, then it transmit to the marriage pool for participating to produce generations.

5.3.2. Crossover

Among different crossover operators [21], the heuristic type is used in this work. In this operator using the fitness values of the two parent chromosomes, the direction of the search is determined. If X and Y are parent chromosomes and X', Y' are offsprings, then the offsprings are made according to the following equations:

$$X' = X + r.(X - Y) \quad (14)$$

$$Y' = X \quad (15)$$

where, r is a random number between zero and one. If the chosen r causes one or more genes of chromosome to be outside of the allowable upper or lower bounds, then is not allowed. In this state, a new random number r is generated and a new offspring is created by Eq. (14).

5.3.3. Mutation

There are different types of mutation functions which are used in the GA [21]. The uniform mutation function is applied in this work. First, according to the mutation probability, the number of variables in the population are selected randomly, then each variable changes according to type of mutation and is replaced in the population. General structure of this operator for number with floating point is defined by:

$$X = (x_1, x_2, \dots, x_m) \xrightarrow{\text{Mutation}} X' = (x'_1, x'_2, \dots, x'_m)$$

$$x_i, x'_i \in [x_i^{lo}, x_i^{hi}] \quad \text{for } i = 1, 2, \dots, m \quad (16)$$

In this mutation, a variable that should be mutated is replaced with a random value in defined range, where r is a random number in the interval between zero and one, with a uniform distribution.

$$x'_i = x_i^{lo} + r.(x_i^{hi} - x_i^{lo}) \quad (17)$$

5.4. Replacement (select next generation) and termination criteria

At the end of each iteration of genetic algorithm, there are two generations of parents and offspring. Among the two generations that includes 2N member, N number of members should be elected to continue the algorithm. Elitist selection method is also used in this work. Thus, most qualified chromosomes will be allowed to be transferred directly to the next generation. Next, the process of evaluation and reproduction for each

chromosome is repeated until the stopping criteria are met. Termination criterion of our algorithm is the maximum number of generations.

6. Simulation results

In this section, we investigate the performance of discussed algorithms for nonlinearity modeling of three-mode heterodyne interferometer in measurement of refractive index shift. The input data for the neural network are two output currents of avalanche photodiodes. In the training phase, the training input vector $P=[I_{APD1}, I_{APD2}]$ is gained by putting the fixed parameters and nonlinear parameters in Eqs. (4) and (5). The target vector is generated by Eq. (8) $T = [\Psi_{n1}]$. The structure of MLPs is (2:12:1) and the training is done in 1000 epochs with the learning rate of 0.01. The Stacking structure is four MLPs network with (4:12:1) structure.

In MLPs and Stacking methods, MSE value is not decreased favorably; however, the network trains in a lot of epochs. Genetic algorithm is set for training the MLPs and Stacking with heuristic crossover 0.8, uniform mutation probability 0.01, 150 chromosomes (population size) in MLPs and 190 chromosomes in Stacking. The algorithm is repeated for 100 generations. The nonlinearity error is simulated by using mathematical rules as reference. The nonlinearity in the testing phase is modeled by MLPs and MLPs-GA as shown in Fig. 7. The main parameters are considered as $|\alpha|=0.02, |\beta|=0.002, \phi_\alpha = \phi_\beta = 0.5rad$. Figure 8 shows the nonlinearity error modeled by Stacking and Stacking-GA, considering the same parameters. According to Eq. (8), the value of nonlinearity error should be decreased in order to get a better modeling, and finally a better measurement of refractive index in membrane of fuel cell. The MSE values for various parameters of the nonlinearity error in testing phase, using each of aforementioned method are listed in Table 1. Results show that the performance of the MLPs-GA and Stacking-GA method for nonlinearity modeling are much better than each of MLPs and Stacking. According to the

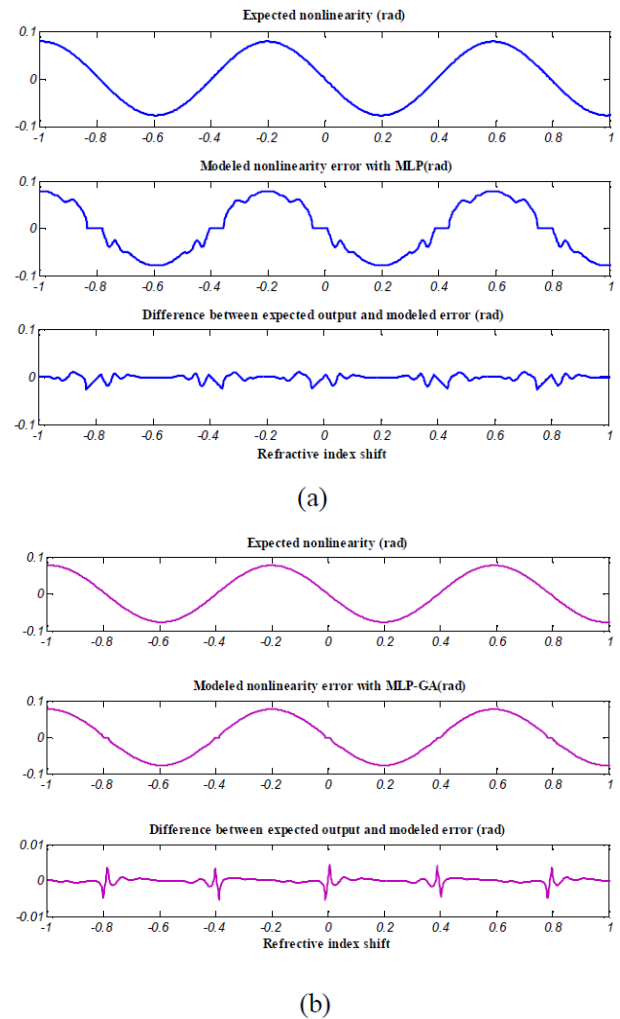


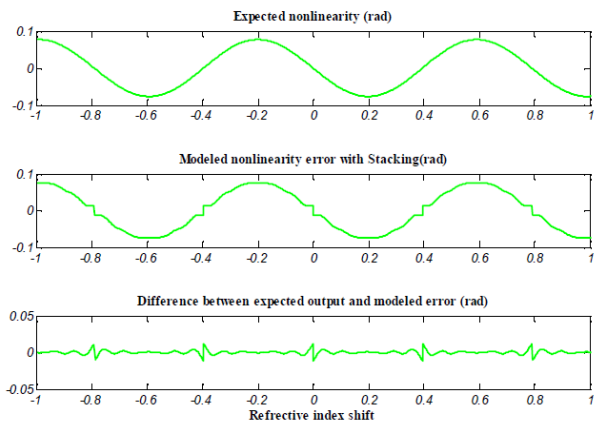
Fig. 7. The nonlinearity error modeling in refractive index determination by (a) MLPs and (b) MLPs-GA; expected nonlinearity (up), the modeled nonlinearity (middle), and the difference between expected and modeled nonlinearity (down).

results, the MSE value for different error parameters is between -46.34dB and -35.61dB for MLPs and between -65.42dB and -52.25dB for stacking method. When we use GA approach, these values are respectively improved to -89.07dB and -70.68dB for MLPs-GA and -121.12dB to -98.58dB for Stacking-GA. By comparing the results and the reported results in [7] which have been extracted from nonlinearity modeling by least mean square (LMS), normalized least mean square (NLMS), affine projection algorithm (APA), and recursive least squares (RLS) methods, it is concluded that by applying the GA, the MSE is

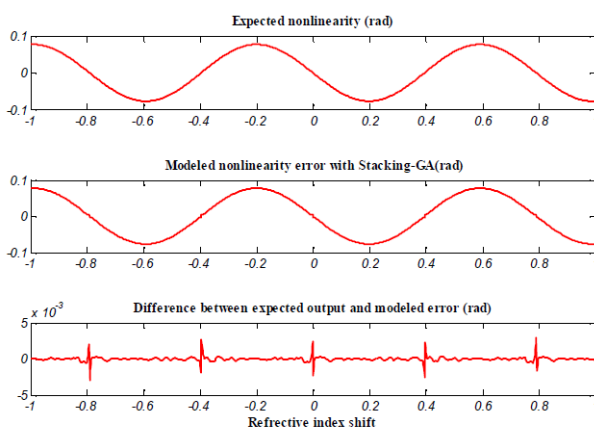
considerably minimized.

Table1. The results of nonlinearity modeling for some error parameters.

$ \alpha $	$ \beta $	ϕ_α (rad)	ϕ_β (rad)	MSE (dB)			
				MLPs	Stacking	MLPs-GA	Stacking-GA
0.02	0.01	0.6	0.5	-44.74	-64.68	-86.12	-118.32
0.02	0.04	0.5	0.5	-46.34	-65.42	-89.07	-121.12
0.02	0.1	0.5	0.6	-35.61	-52.25	-70.68	-98.58
0.04	0.01	0.5	0.5	-37.52	-53.18	-77.34	-104.48
0.01	0.01	0.5	0.45	-45.43	-65.11	-88.53	-117.45
0.01	0.02	0.5	0.5	-40.84	-60.44	-83.62	-114.86
0.02	0.002	0.5	0.5	-42.08	-63.78	-80.88	-110.73



(a)



(b)

Fig. 8. The nonlinearity error modeling in refractive index determination by (a) Stacking and (b) Stacking-GA; expected nonlinearity (up), the modeled nonlinearity (middle), and the difference between expected and modeled nonlinearity (down).

7. Conclusion

In this paper, MLPs and Stacking, MLPs-GA and Stacking-GA have been applied for modeling the nonlinearity error resulting from ellipticity polarization and non-orthogonality of input beam in three-longitudinal-mode laser heterodyne interferometer for refractive index determination of fuel cell membrane. Our methodology adopts a real coded GA strategy and the genetic operators can find optimized weights and biases of the neural networks much better than gradient descent method while they prevent from some problems like premature convergence and falling in local minima. Our main results depicts that genetic algorithm, which is able to search globally, improves the performances of both the MLPs and the Stacking methods in modeling of measurement error in refractive index determination of fuel cell. It has been also shown that the Stacking-GA method modeled nonlinearity better than other approaches. In a special case, the minimum MSE has been obtained to be equal to -121dB.

8. References

1. Yazici M. S., "Hydrogen and fuel cell activities at UNIDO-ICHET", Int. J. Hydrogen Energy 2010, 35: 2754.

2. Thomas S. and Zalbowitz M., *Fuel Cells – Green Power Hand Book*. U.S. Department of Energy, Office of Transportation Technologies, 2010.
3. Kirubakaran A. and Jain R.K., “A review on fuel cell technologies and power electronic interface”, *Renewable and Sustainable Energy Reviews*, 2009, 13: 2430.
4. Motupally S., Becker A.J. and Weidner J.W., “Diffusion of water in nafion 115 membranes”, *J. Electrochemical Society*, 2000, 147: 3171.
5. Tsushim S. and Aotani K., “Magnetic resonance imaging of a polymer electrolyte membrane under water meation”, *Experimental Heat Transfer*, 2009, 22: 1.
6. Waller L., Kim J., Shao-Horn Y. and Barbastathis G., “Interferometric tomography of fuel cells for monitoring membrane water content”, *Opt. Express*, 2009, 17: 16806.
7. Olyae S. Abadi M.S.E., Hamedi S. and Finizadeh F., “Refractive index determination and nonlinearity modeling in fuel cells using laser heterodyne interferometer”, *Int. J. Hydrogen Energy*, 2011, 36: 13255.
8. Quenelle R.C., “Nonlinearity in interferometric measurements”, *Hewlett-Parkard J.*, 1983, 34, 10.
9. Sutton C.M., “Nonlinearity in the length measurement using heterodyne laser Michelson interferometry”, *J. Phys. E: Sci. Instrum.*, 1987, 20: 1290.
10. Olyae S., Yoon T.H., and Hamedi S., “Jones matrix analysis of frequency mixing error in three-longitudinal-mode laser heterodyne interferometer”, *IET Optoelectron.*, 2009, 3: 215.
11. Li Z., Herrmann K. and Pohlenz F., “A neural network approach to correcting nonlinearity in optical interferometers”, *Meas. Sci. Technol.*, 2003, 14: 376.
12. Heo G., Lee W., Choi S., Lee J. and You K., *Adaptive neural network approach for nonlinearity compensation in laser interferometer*. Springer Press, 2007.
13. Olyae S., Ebrahimpour R. and Hamedi S., “Modeling and compensation of periodic nonlinearity in two-mode interferometer using neural networks”, *IETE J. Research*, 2010, 56: 102.
14. Hornik K., Stinchcombe M. and White H., “Multi-layer feed forward networks are universal approximators”, *Neural Networks*, 1989: 2, 359.
15. Sedki A., Ouazar D., and El-Mazoudi E., “Evolving neural network using real coded genetic algorithm for daily rainfall–runoff forecasting”, *Expert Systems with Applications*, 2009, 36: 4523.
16. Wolpert D. H., “Stacked generalization”, *Neural Networks*, 1992, 5: 241.
17. Fogel D. B., “An introduction to simulated evolutionary optimization”, *J. IEEE Trans.*, 1994, 5, 3.
18. Ganatra A., Kosta Y. P., Panchal G. and Gajjar C., “Initial classification through back propagation in a neural network following optimization through GA to evaluate the fitness of an algorithm, *International Journal of Computer Science & Information Technology (IJCSIT)*, 2011, 3, 98.
19. Hertz J., Krogh A. and Palmer R., *An Introduction to the Theory of Neural Computation*, Addison-Wesley, 1991.
20. Whitfield D. and Martin E. H., “New directions in cryptography”, *IEEE Transactions on Information Theory*, 1986, 14: 644.
21. Michalewicz Z., *Genetic Algorithms + Data Structures = Evolution Programs*. Springer-Verlag, New York, 1992.